JOURNAL OF STRUCTURAL BIOLOGY **121,** 356–361 (1998)
ARTICLE NO. SB984003

Growth of Protein 2-D Crystals on Supported Planar Lipid Bilayers Imaged *in Situ* by AFM

Ilya Reviakine, Wilma Bergsma-Schutter, and Alain Brisson[1]

Department of Biophysical Chemistry, GBB, University of Groningen, Nijenborgh 4, 9747 AG Groningen, The Netherlands

Received May 11, 1998, and in revised form May 13, 1998

Theories of crystallization, both in 3-D and 2-D, are still very limited, mainly due to the scarcity of experimental approaches providing pertinent data on elementary phenomena. We present here a novel experimental approach for following, in real time and *in situ,* the process of 2-D crystallization of proteins on solid supports. Using annexin V as a model of a protein binding by affinity to a lipid matrix, we show that 2-D crystals of proteins can be formed on supported planar lipid bilayers (SPBs). Atomic Force Microscopy (AFM) enables the process of 2-D crystal growth to be visualized. The submolecular organization of the crystals was characterized at a resolution of ~ 2 nanometers, and defects, hitherto not observed in protein crystals, were resolved. These results have potential applications in basic and applied sciences.

Key Words: **protein 2-D crystallization; atomic force microscopy; supported planar lipid bilayers; annexin V; crystal growth.**

INTRODUCTION

The possibility of controlling the crystallization of biological macromolecules, both in 3-D and in 2-D, would have obvious interest in the field of structural biology (Giegé and Ducruix, 1992). In the remote field of nanotechnology, the control of the nanometer-scale organization of (macro)molecules containing addressable functional groups and assembled in well-defined patterns on solid surfaces also constitutes a central issue (Special Section of *Science*, 1991). Our objective was to develop a technology for constructing ordered assemblies of proteins, such as 2-D crystals, on solid supports, and to characterize their nanometer-scale organization.

The most reliable methods for crystallizing proteins in 2-D rely either on the incorporation of membrane proteins within lipid bilayers (Kuehlbrandt, 1992), or on the specific anchoring of soluble proteins to lipid monolayers at the air–water interface (Uzgiris and Kornberg, 1983; Brisson *et al.*, 1994). The association of a protein, in a fixed orientation, to a planar substrate seems therefore sufficient for triggering the self-assembly of proteins into 2-D crystals. Since the deposition of membrane-protein 2-D crystals is inappropriate to cover extensive solid surfaces with a homogeneous 2-D crystalline layer, and since the transfer of existing 2-D crystals from an air–water interface to a solid support faces intrinsic difficulties incompatible with the development of a reliable technology (Brisson *et al.*, 1998), we investigated the possibility of growing 2-D crystals, *in situ,* on solid supports functionalized by SPBs (Sackmann, 1996; Watts *et al.*, 1986). SPBs have already received much attention, with applications from cell biology to biosensor technology (Review by Sackmann, 1996).

This novel technology was developed with annexin V as a model protein, for its property of binding specifically to negatively charged lipids, such as phosphatidylserine (PS), in a Ca^{2+}-dependent manner (Review by Demange *et al.*, 1994), and forming 2-D crystals by specific interaction with PS-containing lipid monolayers at the air–water interface (Mosser *et al.*, 1991; Brisson *et al.*, 1991; Voges *et al.*, 1994). AFM (Binnig *et al.*, 1986; Radmacher *et al.*, 1992) was chosen for these experiments, for its unique ability to image biological macromolecules in their native aqueous environment (Schabert *et al.*, 1995; Mueller *et al.*, 1997; Mou *et al.*, 1995; Kuznetsov *et al.*, 1997), with a resolution ranging from tens of microns to angströms.

MATERIALS AND METHODS

Materials. The lipids dioleoylphosphatidylcholine (DOPC) and dioleoylphosphatidylserine (DOPS) were purchased from Avanti Polar Lipids (AL).

Recombinant rat annexin V was expressed in *E. coli* strain JM103 containing annexin V cloned in the expression vector pKK233-2 as described by Swairjo *et al.* (1994), and purified according to Burger *et al.* (1993).

[1] To whom correspondence and reprint requests should be addressed. Fax: (31) 50 363 48 00. E-mail: brisson@chem.rug.nl.

1047-8477/98 $25.00

The buffer contained 2 mM $CaCl_2$, 150 mM NaCl, 10 mM Hepes, 3 mM NaN_3, pH 7.4.

Sample preparation. A lipid mixture containing 80% DOPC and 20% DOPS in chloroform was used in these experiments. To form small unilamellar vesicles (SUVs), lipids were dried under vacuum for 30 min, before being resuspended in buffer at a final concentration of 0.5 mg/ml and sonicated with a tip sonicator. SPBs were formed by deposition of 120 µl of freshly sonicated SUVs onto a cleaved mica surface and incubation for 40 to 60 min at room temperature. The excess of lipids was removed by exchanging the solution covering mica with buffer, and the sample was then installed in the AFM. The microscope was allowed to thermally equilibrate for a minimum of 30 min.

For the experiments focussing on the growth of annexin V 2-D crystals (described in the legend of Fig. 1), 300 µl of a 10 µg/ml annexin V solution were injected into the fluid cell of the AFM, and the microscope was allowed to equilibrate for a further 10 min before imaging.

For the other experiments, 1 ml of a 25 µg/ml annexin V solution was injected into the fluid cell and allowed to stand for 0.5–4 h prior to imaging.

Experiments were performed at room temperature.

Atomic force microscopy. AFM was performed using a Nanoscope IIIa-MultiMode AFM (Digital Instruments, Santa Barbara, CA) equipped with a "J" (120 µm) or an "E" (16 µm) scanner. Mica plates were glued onto metal disks using double-sided tape, and installed into a contact mode fluid cell equipped with an O-ring to allow exchange of buffers.

Images were recorded in the constant force mode using oxide-sharpened silicon nitride tips mounted on cantilevers with nominal force constant of 0.06 N/m, at scanning rates of 3–8 Hz. The scan angle was 90°. The force used was maintained close to 0.1 nN. Both trace and retrace signals were acquired and compared by aligning them and calculating a difference image. For all images shown here, both signals were similar. The only treatment applied to AFM images was flattening (NanoScope Reference Manual, 1996), except for Figs. 2D and 2E.

Averaging of AFM images of annexin V trimers. Averaging of AFM images of annexin V trimers was performed using procedures commonly used in electron microscopy (EM) and referred to as single particle averaging (Frank, 1990). Subareas (257 × 257 nm) from (400 × 400 nm) AFM images were selected using the Zoom function on the NanoScope software (NanoScope Reference Manual, 1996) and 72 images (64 × 64 pixel size) of annexin V trimers located at the threefold symmetry centers on the p6 lattice were extracted and processed using IMAGIC software (van Heel and Keegstra, 1981). Individual images were translationally aligned using a sixfold averaged image of one trimer as a reference, and classified into nine distinct classes. The members of each class were summed and threefold rotational symmetry was imposed to the sums.

Cryoelectron crystallography of annexin V 2-D crystals. Annexin V 2-D crystals were grown on DOPS-containing lipid monolayers at the air–water interface and transferred to holey carbon grids, as described in Brisson *et al.* (1998). The specimens were prepared for cryo-EM by quick-freezing into cooled liquid ethane (Dubochet *et al.*, 1982); EM was performed using a CM-120 Philips microscope. Fourier transforms of the best images exhibited peaks extending to better than 2 nm. Projection maps calculated by standard procedures presented reliable structural details up to 1.5 nm.

RESULTS AND DISCUSSION

As the presence of SPBs continuously covering solid surfaces was a prerequisite to studies of protein crystallization, their formation was first characterized by AFM. The results of these experiments showed that SPBs could be formed on mica or silicon by fusion of SUVs made of lipids in fluid phase, and that SPBs consisted of almost perfectly flat single lipid bilayers covering completely the substrate surface (to be published elsewhere).

When annexin V was added to PS-containing SPBs in the presence of Ca^{2+} ions, circular crystalline domains of micrometer-diameter covering the lipid surface were observed by AFM within 10 min (Fig. 1). All of the observed domains were crystalline. These domains were 2.6 ± 0.2 nm (n = 16) higher than the lipid surface. This height is smaller than the known thickness, about 3.5 nm, of membrane-bound annexin V molecules (Brisson *et al.*, 1991; Huber *et al.*, 1990); the origin of this height difference is still unclear. The circular domains observed by AFM are thus 2-D crystals made of a monomolecular layer of annexin V specifically bound to a PS-containing SPB.

The radial growth of these domains was followed in real time, as depicted in Fig. 1. In the experimental conditions presented here, the average growth rate was 0.005 $\mu m^2/s$. The complete SPB surface eventually became covered with crystalline domains separated by grain boundaries (Figs. 1D–1F and 2A). The time required for homogeneously dispersed crystalline domains to form a 2-D continuum—half an hour in the conditions of Fig. 1—provides a direct explanation of the lag period separating the onset of protein absorption and the establishment of a measurable lateral rigidity, as observed on similar systems at the air–water interface (Vénien-Bryan *et al.*, 1998).

Our working hypothesis is that 2-D crystals grow by incorporating at their edges lipid-bound annexin V molecules—or annexin V trimers (see below)—diffusing in the lipid plane. The fact that the lipid surface separating the crystalline domains seems to be devoid of annexin V molecules suggests that the rate of crystal growth is limited either by the Ca^{2+}-mediated binding of annexin V to the SPB or/and by the formation of annexin V trimers. Although information on the nucleation step is still lacking, the present data suggest that nucleation is a fast process since the average rate of crystal growth remained constant throughout the experiment. The experimental approach presented here provides a unique way to assess the respective influence of basic parameters such as diffusion of the protein in the 3-D volume, binding interaction, and diffusion of protein–lipid complexes in 2-D, on the formation of 2-D crystals. A comprehensive model of 2-D crystal growth is expected to emerge from this novel approach.

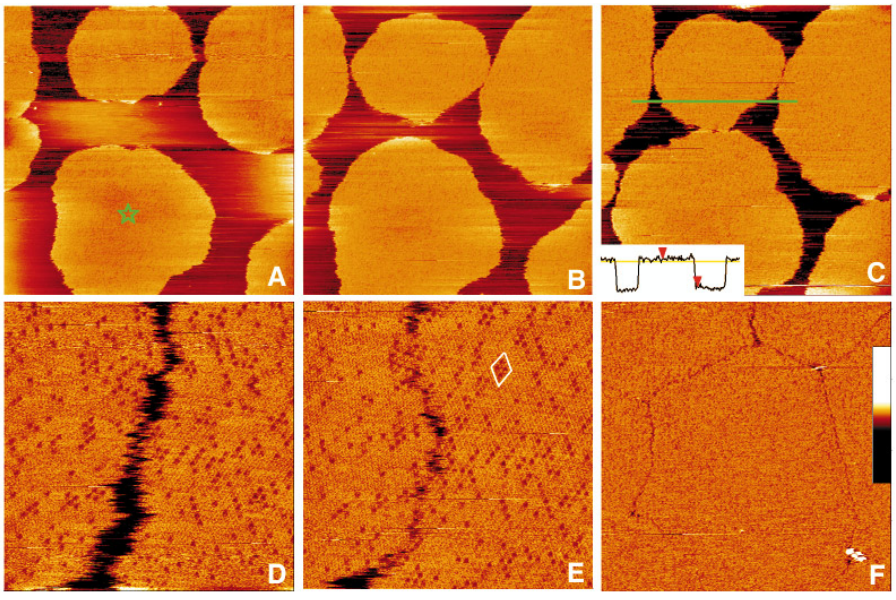

FIG. 1. Growth of crystalline domains of annexin V on a PS-containing SPB on mica, imaged by AFM. Successive images of the same area are presented in A–C and in D, E. Time after injection of annexin V in the fluid cell: (A) 19 min; (B) 23 min; (C) 26 min; (D) 29 min; (E) 31 min; (F) 34 min. (A) Circular domains (one domain is labeled with a green asterisk) are homogeneously distributed over the SPB surface. These domains grow and coalesce from A to E. (C) The height profile measured along the green line is shown in the inset. The three crystalline domains are of identical height and the lipid surface is flat. The height measured between the two red arrowheads is 2.6 nm. Scan size, A–C: 5 μm. (D, E) Enlarged view of a grain boundary forming between two adjacent domains. Between (D) and (E), the gap between the two domains decreases in width, which corresponds to the incorporation of incoming molecules to the crystals. Vacancies, or holes, are seen within the lattice (a lozenge surrounds four such vacancies; see Fig. 3B). The overall process seems highly dynamical, as holes form or disappear with time. Some exchange of material is also seen to occur between the two facing domains. Scan size: 870 nm. (F) Crystalline domains cover completely the mica surface and are separated from each other by grain boundaries. Scan size: 4.1 μm. Z-scale (shown in (F)): 10 nm from black to white.

The crystalline organization of the annexin V assemblies could be revealed by AFM at a resolution of ~ 2 nanometers (Figs. 1D, 1E, and 2). The crystals exhibit the symmetry of the plane group p6 and are similar to one of the crystal forms already described by EM (Brisson *et al.*, in press; Voges *et al.*, 1994) and X-ray surface diffraction (Lenne, 1988) on lipid monolayers at the air–water interface. In this crystal form, six annexin V trimers are arranged with p6 symmetry, while a seventh trimer is located, in a

FIG. 2. AFM images of annexin V 2-D crystals grown on DOPS-containing SPBs. (A) Sample imaged after ~ 4 h incubation. The lipid bilayer is covered by 2-D crystalline domains separated by grain boundaries. Scan size: 1.5 μm. (B) Area (257 × 118 nm) of an annexin V crystal. The white box (right) surrounds six annexin V trimers located at the vertices of a hexagon; a seventh trimer is located at the hexagon's center. In the left box, the trimers have been labeled alternatively with a blue and a green dot; the "blue" trimers and the "green" trimers are related by a 60°-rotation perpendicular to the crystal plane. The lattice vectors are 30 nm along the direction closest to the vertical and 25 nm for the two others. The lattice vector lengths presented variations between images, which most likely resulted from drift and distorsions due to the use of an O-ring. (C) 2-D projected structure of membrane-bound annexin V at 1.5 nm resolution, calculated by cryoelectron crystallography of 2-D crystals grown on lipid monolayers at the air–water interface. Scale bar: 10 nm. Annexin V molecules are viewed from the aqueous solution. Six annexin V trimers have also been labeled in blue or green, in order to facilitate the comparison between the direct, unprocessed AFM image (B) and this noise-filtered 2-D EM map. The domains 1, 2, 3, 4 (numbered after Huber *et al.*, 1990) are indicated for one annexin V molecule. Image size: 36 × 36 nm. In the AFM images, the connecting regions between the trimers, made by domains 3, dominate the p6-lattice and are higher by ~ 0.45 nm than the upper flat surface of the (1, 4) module. The density corresponding to domain 2 is absent in AFM images, which indicates that domain 2 is lower than the other three domains and is not accessible to the AFM tip. The surface topology revealed by AFM is thus strikingly similar to that of the soluble form of annexin V (Huber *et al.*, 1990; Sopkova *et al.*, 1993; Swairjo *et al.*, 1995), which suggests that the molecule keeps its slightly curved shape upon membrane binding. These results deviate from the 3-D structure calculated from negatively stained EM data, in which domain 2 was proposed to be the furthest from the membrane and domain 3 the closest (Voges *et al.*, 1994). (D, E) Averaged AFM images of annexin V trimers in the two possible orientations, related by a 60°-rotation (see Materials and Methods). (D) Obtained by summing two of the 9 classes, accounting for ~25% of the data set, which corresponded distinctly to one orientation of the trimers (colored in blue in B). (E) Obtained by summing three classes, accounting for ~30% of the data set, which corresponded to the other, green, orientation. The resolution observed here is consistent with the resolution of 2.3 nm calculated from Fourier transforms of the best AFM images (data not shown). It is likely that the resolution is limited by drift due to the use of an O-ring and by the tip size, as suggested by preliminary results using sharper tips. Image size: 32 × 32 nm.

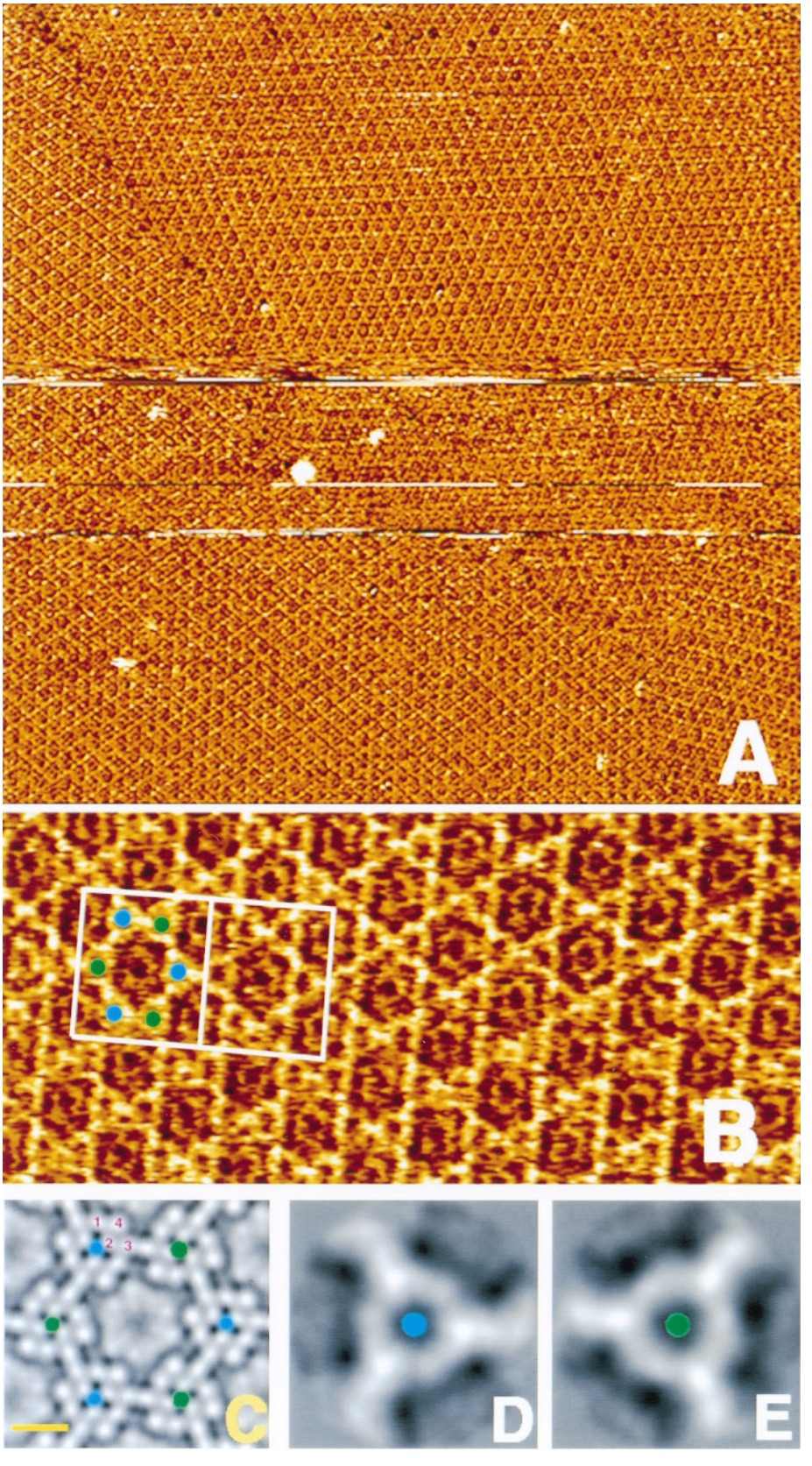
A
B
1 4
2 3
C
D
E

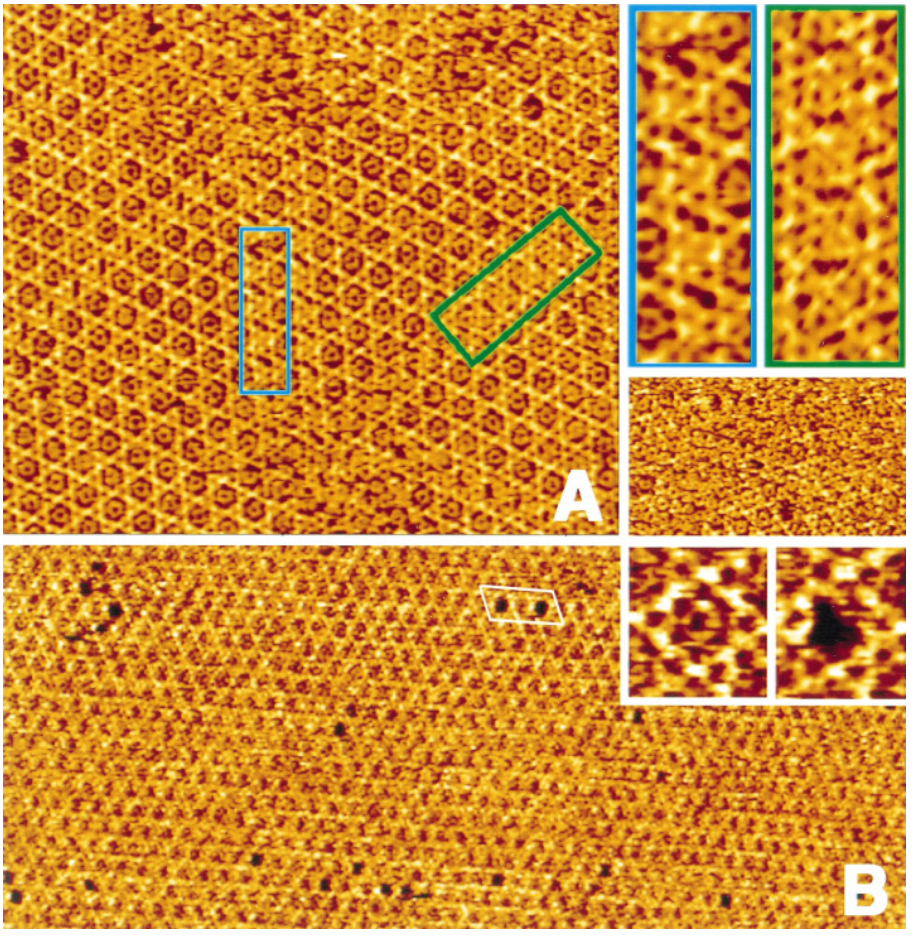

FIG. 3. Defects in annexin V 2-D crystals. (A) Several types of defects can be distinguished within, and also between, the crystalline areas. Examples of defects within the crystalline areas are indicated by a blue and a green box (2.2× enlarged views in the two upper insets). These defects present characteristic zipper-like patterns, accommodating for slight shifts between growing crystals. Bottom inset: close-packed assembly of annexin V trimers found between some crystalline areas, supporting the hypothesis that annexin V trimers constitute the building motifs of the 2-D ordered arrays (Voges *et al*., 1994; Brisson and Lewit-Bentley, 1996). Image size: 546 × 458 nm. (B) Vacancies within some crystalline areas are imaged by AFM as characteristic dark spots or holes (a white parallelogram surrounds two such holes; see also Figs. 1D and 1E with a lozenge surrounding four such holes in Fig. 1D). These holes correspond to the absence of the central annexin V trimer at the (pseudo) sixfold symmetry center of the lattice. Image size: 0.43 × 1.1 μm. Insets: hexagonal arrangement of annexin V trimers, without the central trimer (right) and with the central trimer (left).

noncrystallographic manner, at the sixfold symmetry center (these crystals are thus pseudo-p6 crystals, but referred to here as p6 crystals for simplicity) (Figs. 2B and 2C). The seven trimers of annexin V were clearly resolved on AFM images, in their physiological environment (Figs. 2 and 3). A close comparison of the annexin V structures obtained by AFM (Figs. 2B, 2D, and 2E) and EM (Fig. 2C) reveals striking similarities and emphasizes the intrinsic high-contrast of unprocessed AFM images of macromolecules in aqueous solutions (Fig. 2B) (Schabert *et al*., 1995; Mueller *et al*., 1997; Mou *et al*., 1995; Kuznetsov *et al*., 1997). The lateral resolution of AFM images, ~ 2 nm, enables the two modules characteristic of annexins, consisting of domains (1, 4) and (2, 3), respectively, to be resolved (numbering after Huber *et al*., 1990) (Figs. 2C–2E). In addition, new details were obtained on the surface topology of membrane-bound annexin V, which is not accessible by either electron or X-ray crystallography (see Figure legend).

These results emphasize the similarity between SPBs and lipid monolayers as supports of protein 2-D crystallization. It is therefore expected that other proteins will crystallize on SPBs, as preliminary experiments indeed indicate for streptavidin on SPBs containing biotinylated lipids (data not shown). The formation of ordered arrays of the B_5 domain of cholera toxin on lipid bilayers has also been reported (Mou *et al*., 1995); however, it was not demonstrated whether these arrays were true 2-D crystals, as is the case for annexin V, or only close-packed assem-

blies which are commonly found with annular-shaped structures like B_5 (Mosser and Brisson, 1991). It is noteworthy that the annexin V 2-D crystals did not exhibit any tendency toward 3-D crystal growth by epitaxy. The upper surface of annexin V crystals is thus ideally flat for the deposition of an additional molecular layer, by either covalent interaction or affinity with modified annexins, opening the way for a layer by layer building of supramolecular assemblies.

A close investigation of the morphology of annexin V crystals revealed several types of defects within the crystalline domains (Fig. 3), in addition to the grain boundaries present between crystalline domains (Figs. 1D–1F and 2A). Defects of the first type join, in a zipper-like manner, two neighboring crystals with identical lattice orientations but slightly shifted relative to each other. To our knowledge, this is the first direct demonstration of the existence of such defects in protein 2-D crystals, which present analogy with stacking faults in solids. Defects of the second type consist of vacancies randomly distributed in crystals (Figs. 1D, 1E, and 3B). These vacancies are located at the sixfold symmetry centers and correspond to the absence of the noncrystallographic seventh trimer. The number of vacancies decreased with time (compare Figs. 1D, 1E and Fig. 2A) , and almost no vacancies were visible after incubation for several hours. This indicates that the central, seventh trimer, is not required for the p6 crystal to be formed and that an extra trimer can be added at a later stage, most likely by recruitment of annexin V molecules from the solution. The ability to visualize crystalline defects *in situ* will certainly lead to an improved understanding of crystal growth and open interesting possibilities for growing large 2-D crystals amenable to high-resolution structure determination by grazing angle X-ray or neutron diffraction.

This report demonstrates that SPBs form flat 2-D surfaces which are able to support the 2-D crystallization of macromolecules by molecular recognition and self-assembly. The ability to follow the growth of protein 2-D crystals on SPBs, in a controlled fashion, and to characterize their submolecular organization, *in situ* , by AFM, offers exciting opportunities in basic science for investigating crystallization processes, and provides an adequate technology for fabricating protein-containing biofunctional surfaces.

We thank G. Oostergetel for his critical reading of the manuscript, B. Seaton, T. Mealy, and B. Pepinsky for the generous gift of cell lines containing the annexin V clone, E. Boekema for his help with image processing, and A. Arkema for her technical asssistance. I.R. is recipient of a Ubbo Emmius PhD fellowship from the University of Groningen. This work was supported by the Netherlands Foundation for Chemical Research (SON) and the EU (Grant BIO4 CT96-0083 to A.B.).

REFERENCES

Binnig, G., Quate, C. F., and Gerber, Ch. (1986) Atomic force microscope, *Phys. Rev. Lett.* **56**(9), 930–933.

Brisson, A., Lambert, O., and Bergsma-Schutter, W. (1998) Two-dimensional crystallization of soluble proteins on planar lipid films: A practical approach, *in* Ducruix, A., and Giegé, R. (Eds.), Crystallization of Nucleic Acids and Proteins: A practical Approach, in press, Oxford Univ. Press.

Brisson, A., and Lewit-Bentley, A. (1996) A common trimer of annexin V as a basic unit in 2D and 3D crystal forms, *in* Seaton, B. A. (Ed.), Annexins: Molecular Structure to Cellular Function, pp. 43–52, Chapman and Hall, New York.

Brisson, A., Mosser, G., and Huber, R. (1991) Structure of soluble and membrane-bound human annexin V, *J. Mol. Biol.* **220,** 199–203.

Brisson, A., Olofsson, A., Ringler, P., Schmutz, M., and Stoylova, S. (1994) Two-dimensional crystallisation of proteins on planar lipid films and structure determination by electron crystallography, *Biol. Cell* **80,** 221–228.

Burger, A., Berendes, R., Voges, D., Huber, R., and Demange, P. (1993) A rapid and efficient purification method for recombinant annexin V for biophysical studies, *FEBS Lett.* **329,** 25–28.

Demange, P., Voges, D., Benz, J., Liemann, S., Gottig, P., Berendes, R., Burger, A., and Huber, R. (1994) Annexin V: The key to understanding ion selectivity and voltage regulation, *Trends Biochem. Sci.* **19,** 272–276.

Dubochet, J., Lepault, J., Freeman, P., Berriman, J. A., and Homo, J.-C. (1982) Electron microscopy of frozen water and aqueous solutions, *J. Microsc.* **128,** 219–237.

Frank, J. (1990) Classification of macromolecular assemblies studied as single particles, *Quat. Rev. Biophys.* **23,** 281–329.

Giegé, R., and Ducruix, A. (1992) An introduction to the crystallogenesis of biological macromolecules, *in* Ducruix, A., and Giegé R. (Eds.), Crystallisation of Nucleic Acids and Proteins: A Practical Approach, pp. 1–18, Oxford Univ. Press.

van Heel, M. G., and Keegstra, W. (1981) IMAGIC: A fast, flexible and friendly image analysis system, *Ultramicroscopy* **7,** 113–130.

Huber, R., Roemisch, J. M., and Paques, E. P. (1990) The crystals and molecular structure of human annexin V, an anticoagulant protein that binds to calcium and membranes, *EMBO J.* **9,** 3867–3874.

Kuehlbrandt, W. (1992) Two dimensional crystallization of membrane proteins, *Quart. Rev. Biophys.* **25,** 1–49.

Kuznetsov, Yu. G., Malkin, A. J., Land, T. A., DeYoreo, J. J., Barba, A. P., Konnert, J., and McPherson, A. (1997) Molecular resolution imaging of macromolecular crystals by atomic force microscopy, *Biophys. J.* **72,** 2357–2364.

Lenne, P.-F. (1998) PhD dissertation, Grenoble.

Mosser, G., and Brisson, A. (1991) Structural analysis of two-dimensional arrays of cholera toxin B subunit, *J. Electr. Microsc. Techn.* **18,** 387–394.

Mosser, G., Ravanat, C., Freyssinet, J.-M., and Brisson, A. (1991) Sub-domain structure of lipid-bound annexin-V resolved by electron image analysis, *J. Mol. Biol.* **217,** 241–245.

Mou, J., Yang, J., and Shao, Z. (1995) Atomic force microscopy of cholera toxin B oligomers bound to bilayers of biologically relevant lipids, *J. Mol. Biol.* **248,** 507–512.

Mueller, D. J., Amrein, M., and Engel, A. (1997) Adsorption of biological macromolecules to a solid support for scanning probe microscopy, *J. Struct. Biol.* **119,** 172–188.

NanoScope Command Reference Manual (1996) Digital Instruments, Version 4.11.

Radmacher, M., Tillman, R. W., Fritz, M., and Gaub, H. E. (1992)

From molecules to cells: imaging soft samples with atomic force microscope, *Science* **257,** 1900–1905.

Sackmann, E. (1996) Supported membranes: Scientific and practical applications, *Science* **271,** 43–48.

Schabert, F. A., Henn, C. H., and Engel, A. (1995) Native *Escherichia coli* OmpF porin surfaces probed by atomic force microscopy, *Science* **268,** 92–94.

Sopkova, J., Renouard, M., and Lewit-Bentley, A. (1993) The crystal structure of a new high-calcium form of annexin V, *J. Mol. Biol.* **234,** 816–825.

Special Section "Engineering a Small World" (1991) *Science* **254,** 1300–1341.

Swairjo, M. A., Concha, N. O., Kaetzel, M. A., Dedman, J. R., and Seaton, B. A. (1995) Ca^{2+}-bridging mechanism and phospholipid head group recognition in the membrane-binding protein annexin V, *Nature Struct. Biol.* **11,** 968–974.

Swairjo, M. A., Roberts, M. F., Campos, M.-B., Dedman, J. R., and Seaton, B. A. (1994) Annexin V binding to the outer leaflet of small unilamellar vesicles leads to altered inner-leaflet properties: ^{31}P- and ^{1}H-NMR studies, *Biochemistry* **33,** 10944–10950.

Vénien-Bryan, C., Lenne, P.-F., Zakri, C., Renault, A., Brisson, A., Legrand, J.-F., and Berge, B. (1998) Characterization of the growth of 2D protein crystals on a lipid monolayer by ellipsometry and rigidity measurements coupled to electron microscopy, *Biophys. J.* **74**, in press.

Voges, D., Berendes, R., Burger, A., Demange, P., Baumeister, W., and Huber, R. (1994) Three-dimensional structure of membrane bound annexin V—A correlative electron microscopy-X-ray crystallography study, *J. Mol. Biol.* **238,** 199–213.

Uzgiris, E. E., and Kornberg, R. D. (1983) Two-dimensional crystallization technique for imaging macromolecules, with application to antigen-antibody-complement complexes, *Nature* **301,** 125–129.

Watts, T. A., Gaub, H. E., and McConnell, H. M. (1986) T-cell-mediated association of peptide antigen and major histocompatibility complex protein detected by energy transfer in an evanescent wave-field, *Nature* **320,** 179–181.